RESEARCH ARTICLE

Experimental study on mixed pyrolysis of biomass and coal gangue

Liping Wang[1], Enliang Ren[1], Tao Tang[2, 3, *], Zhongyi Qu[4], Xia Liu[1], Xiaoyu Gao[1], Wei Yang[1]

[1]College of Water Conservancy and Civil Engineering, Inner Mongolia Agricultural University, Hohhot, Inner Mongolia, China. [2]CAS Key Lab of Low-Carbon Conversion Science & Engineering; [3]State Key Laboratory of Low Carbon Catalysis and Carbon Dioxide Utilization, Shanghai Advanced Research Institute, Chinese Academy of Sciences, Shanghai, China. [4]School of Energy and Environment, Inner Mongolia University of Science and Technology, Baotou, Inner Mongolia, China.

Received: June 24, 2024; **accepted:** September 13, 2024.

Energy is the material basis for human survival and development. Coal gangue is the solid waste generated in coal mining and washing. How to use energy efficiently and cleanly and constantly innovate the way of energy and material utilization has always been the research direction in various countries. In this study, the co-pyrolysis characteristics of biomass and gangue as well as their influences on pyrolysis products were studied. The variations of sample weight, structure, and pyrolysis gas at various pyrolysis temperatures were investigated for biomass, gangue, and their combination at different mixing ratios. The results showed that increase of temperature increased pyrolysis degree and mass loss, while increase of biomass proportion increased the intensity of the main pyrolysis peak of derivative thermogravimetric analysis (DTG) curve. Co-pyrolysis effectively inhibited the precipitation of total gas and total amounts of CO_2, CO, and CH_4 gases produced when the pyrolysis of coal gangue to biomass ratio reached 15% to 85% (CG15SS85), which were about 62.98%, 52.82%, and 61.9%, respectively, lower than those of the traditional pyrolysis of biomass at 100% (SS100) to charcoal. The specific surface area of biochar was linearly and positively correlated with adsorption capacity. As temperature increased, biochar pore volume and specific surface area were increased with no obvious correlation between specific surface area and total pore volume. The results of this research provided certain theoretical guidance and technical support for the preparation of biochar by the pyrolysis of biomass and gangue, alleviation of energy shortage, and improvement of environmental conditions.

Keywords: coal gangue; biomass; pyrolysis; thermogravimetric analysis; pore structure.

***Corresponding author:** Tao Tang, CAS Key Lab of Low-Carbon Conversion Science & Engineering; State Key Laboratory of Low Carbon Catalysis and Carbon Dioxide Utilization, Shanghai Advanced Research Institute, Chinese Academy of Sciences, Shanghai 201210, China. Email: tangt@sari.ac.cn.

Introduction

Energy is essential for human survival and development. With the development of societies, human demand for energy continues to rise. Fossil fuels are consumed in large quantities, and serious problems such as energy shortage and environmental pollution are created [1]. In China, coal is the main source of energy. Gangue is a solid waste generated during the mining and washing of coal [2], which contains high amounts of ash and low calorific value and is difficult to burn [3, 4]. Hundreds of millions of tons of coal gangue are discharged every year [5], resulting in

waste of resources along with other problems. Biomass has large reserves, wide distribution, and low pollution [6]. Coal gangue and biomass have complementary characteristics, and the mixed pyrolysis of coal gangue and biomass provides a new approach for their comprehensive utilization [7]. This method can save energy and be conducive to environmental protection. Its pyrolyzed solid product, biochar, is extensively applied in different fields such as soil improvement to increase soil fertility and improve plant growth environment in agriculture [8]. However, limited research has been conducted on how to improve the pyrolysis benefits of gangue, biomass, biochar, and pyrolysis gas after pyrolysis.

Co-pyrolysis of gangue and biomass is defined as a series of physical and chemical reactions occurring under isolating air or oxygen [9]. Common pyrolysis analysis methods include thermogravimetric analysis (TG) and differential scanning calorimetry (DSC) [10-12]. Many factors have been found to affect pyrolysis such as particle size, heating rate, sample volume, mixing ratio, *etc.* [13-14]. Gong *et al*. experimentally showed that faster heating rates increased the weight loss rates of the samples at the same temperature and enhanced the released heat energy [15]. In terms of the characteristics of coal gangue and biomass, the mixture with highly volatile biomass could effectively promote pyrolysis reaction, while high ash contents could fix fine ash in the biomass and reduce dust [16]. Bi *et al*. developed a pyrolysis reaction model for biomass and gangue and showed that the addition of biomass affected the gas release law of gangue pyrolysis, such that small amounts of biomass could significantly decrease the initial decomposition rate of gangue [17]. Howanie *et al*. found that pyrolysis co-gasification had a synergistic effect and effectively improved gasification activity [18]. Many researchers have studied the pyrolysis of gangue and biomass, but research on the surface morphology and adsorption characteristics of biochar after pyrolysis is still in the initial stage. Wei showed that the source and pyrolysis temperature of biochar had significant influences on its morphology and pore structure. It was also found that the pore structure characteristics of different substances under the same conditions were different, and pyrolysis temperature also significantly affected the physical, chemical, and structural properties of biochar [19]. Lu *et al*. applied nitrogen and carbon dioxide as adsorbates and calculated pore size range and quantified pore volume by models of calculation model of pore size distribution for mesoporous and macroporous (BJH), simulation of pore volume by density functional theory (DFT), and Frenkel-Halsey-Hill fractal model (FHH) [20]. It is urgent to analyze the characteristics of the biochar produced after pyrolysis, which is also a major method for judging the synergistic benefits of gangue and biomass pyrolysis. The previous studies revealed that different researchers had carried out relevant research on the processes and products of pyrolysis. However, no comprehensive research has been conducted on the whole pyrolysis process and products.

This research investigated thermogravimetric analysis - derivative thermogravimetric analysis (TG-DTG) curves, weight loss changes, and gas products of gangue and biomass pyrolysis using thermogravimetric analysis combined with thermal chromatography-mass spectrometry. The adsorption and morphology of biochar with different mixing ratios after pyrolysis were identified, while pyrolysis law and biochar performance of gangue and biomass were revealed. Further, the pyrolysis process from the beginning to product and from macro to micro was systematically discussed. The research laid in using graduate materials and coal gangue to mix pyrolysis characteristics and products, and developed high-value utilization schemes for recovering gas generated by pyrolysis and using biochar as pyrolysis product to produce functional materials.

Materials and methods

Preparation of test samples

Coal gangue (CG) was collected from Shenhua Baotou Wanli No. 1 Mine, Baotou, Inner Mongolia, China. Biomass (SS) selection of sunflower straw was obtained from Wuyuan County, Inner Mongolia, China. The gangue powder was sieved through 0.106 mm pores, and sunflower straw was dried, crushed, and sieved through 0.106 mm pores for later use. Sifted test materials were dried at 105℃ for 2 hours before the elemental compositions of samples were checked using ADQ-3E ore element analyzer (Shandong Shantai Intelligent Equipment Co., LTD, Shandong, China) and the moisture, ash, volatile content and fixed carbon of the samples were determined using YGF-3 automatic industrial analyzer (Zhongchuang Instrument, Hebi, Henan, China). 20 mg straw and coal gangue were dried at 105℃ to constant weight, and then were burned at 1,200℃ with pure oxygen followed by reducing temperature to 500℃. The sample was sealed in tinfoil and silver boat by the element analyzer sample package tool. The wrapped sample was pressed into shape by the element analyzer sample forming tool, and then loaded into the elemental analyzer. The components of C, H, O, N were determined through the difference reduction using Macro cube element analyzer (Elementar, Langenselbold, Germany). The results were calculated as follows.

Ash + Total nitrogen + Total carbon + Total oxygen + Total hydrogen = 100%

Pyrolysis test

Pyrolysis tests were performed on a Sta449 F3-Qms type thermal analysis-mass spectrometer (Netzsch, Waldkraiburg, Germany) coupled with QMS 403 mass spectrometer to obtain TG-DTG curves and mass spectra. In addition to detecting the weight change and thermal effects of the samples, the evolved gases were identified and quantified in the same measurement. Five treatments were set based on coal gangue to biomass mass ratio as analytical samples including 100% of CG (CG100), 100% of SS (SS100), 10%:90% of CG:SS (CG10SS90), 5%:95% of CG:SS (CG5SS95), and 15%:85% of CG:SS (CG15SS85). The weight of each sampling was 20 mg. Argon gas was adopted as protective gas. Heating rate was set to 10℃/min with the final temperature of pyrolysis as 800℃. The residence time was adjusted at 1 hour. The pyrolyzed sample was soaked in 200 mL of 1 mol/L hydrochloric acid solution for 10 hours to remove ash substances such as calcium carbonate from the carbonized samples and centrifuged at 4,500 rpm for 20 min to remove the remaining hydrochloric acid solution. The sample was washed with deionized water repeatedly until neutral pH was reached before being dried at 70℃ for 24 hours. Analysis of pore and morphology were performed on pyrolysis samples carbonized with gangue and biomass at different pyrolysis temperatures of 400℃ and 800℃.

Analysis of biochar adsorption and surface morphology

Biochar adsorption-desorption was studied using Autosorb-iQ physical adsorbent instrument (Anton Paar, Graz, Austria). Degassing was undertaken using vacuum at 300℃ for 6 hours to remove guest molecules such as water. N_2-CO_2 adsorption and desorption tests were performed in 77.35 K liquid nitrogen (-196°C) with the pressure range between 0.005 – 0.999P/P_0. The specific surface area was simulated using the equation of multimolecular layer adsorption theory (BET) in a linear phase at P/P_0 < 0.3 [21]. BET equation is based on Langmuir isothermal adsorption theory and was expressed as equation (1) below. The total pore volume was calculated by BJH simulation.

$$V = \frac{V_m pC}{(p_s - p)[1 - (P/p_s) + C(p/p_s)]} \quad (1)$$

where *V* was the total volume of adsorbed gas under equilibrium pressure *P*. V_m was the volume of required gas when the first layer covered catalyst surface. *P* was adsorbed gas pressure when it equilibrated at adsorption temperature. *Ps* was saturated vapor pressure. *C* was a constant related to adsorption.

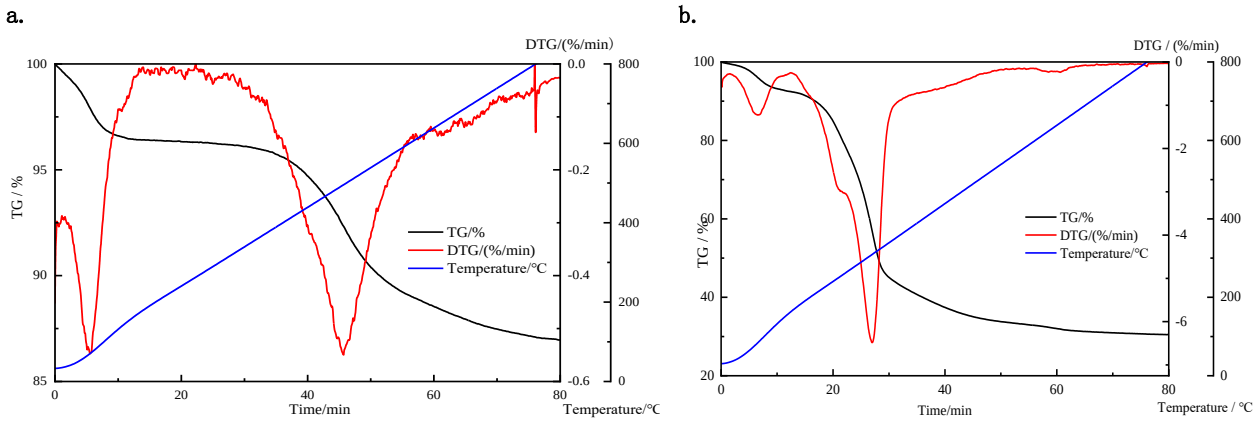

Figure 1. TG-DTG curves of CG100 and SS100 pyrolysis. **a.** coal gangue pyrolysis. **b.** biomass pyrolysis.

Biochar scanning electron microscopy (SEM) images were captured using a Gemini SEM (ZEISS, Oberkochen, Germany). The samples were dried at 75°C for more than 10 hours. The sample surfaces were kept clean. SEM images of typical samples were recorded at 1,000X (10 µm) magnification.

Results and discussion

Analysis of pyrolysis characteristics of biomass and coal gangue

The results showed that the first stage of CG100 pyrolysis at 0 - 185°C was water evaporation stage, which mainly included drying and dehydration with the mass loss rate of 3.66%. The second stage at 185 - 603°C was volatile combustion stage where DTG curve showed fluctuation. At temperatures of higher than 387°C, TG curve changed greatly, sample weight was decreased rapidly, and mass loss rate was about 7.84%. This was the main stage of gangue mass loss and the peak value of DTG was about 457°C. The third stage at 603 - 800°C was fixed carbon ignition stage where DTG curve boundary was multi-peaked, and the curve increase was slow. CG100 was further pyrolyzed to form coke, and mass loss was about 1.55% (Figure 1a). SS100 was dehydrated and dried in the temperature range of 0 - 136°C, while weight loss was observed due to dehydration. The secondary peak of DTG curve appeared at about 66°C with the weight loss rate of 7.89%. When temperature was increased to about 140°C, water evaporation was basically finished. In the second stage at 187-350°C, significant weight loss occurred, and cellulose, hemicellulose, and lignin were decomposed at the same time. The polymerization degrees of cellulose and hemicellulose reduced the cracking of polymer chains resulting in depolymerization to form monomers. Chemical bonds were broken and rearranged. A large amount of heat was absorbed, and pyrolysis products were formed through various free radical and rearrangement reactions. TG curve dropped sharply, the main peak-to-peak temperature of DTG curve was about 270°C. The mass loss rate of this stage was about 46.88%, which was the main stage of SS100 pyrolysis. Weight loss in the third stage at 350-800°C was due to the thermal decomposition of remaining lignin, and weight loss rate was about 10.24%. From 600°C to the end of the test, TG-DTG curve presented insignificant changes and coke continued to decompose, producing carbon-rich solid residues, which entered carbonization stage and the whole process was slow (Figure 1b). The results demonstrated that the main quality loss of CG100 and SS100 occurred in the second stage. The total pyrolysis loss rates of SS100 and CG100 were about 69.52% and 13.04%, respectively. The main peak of SS100-DTG curve appeared earlier than that of CG100 and peak occurrence interval was long, which might be the reason that the volatile

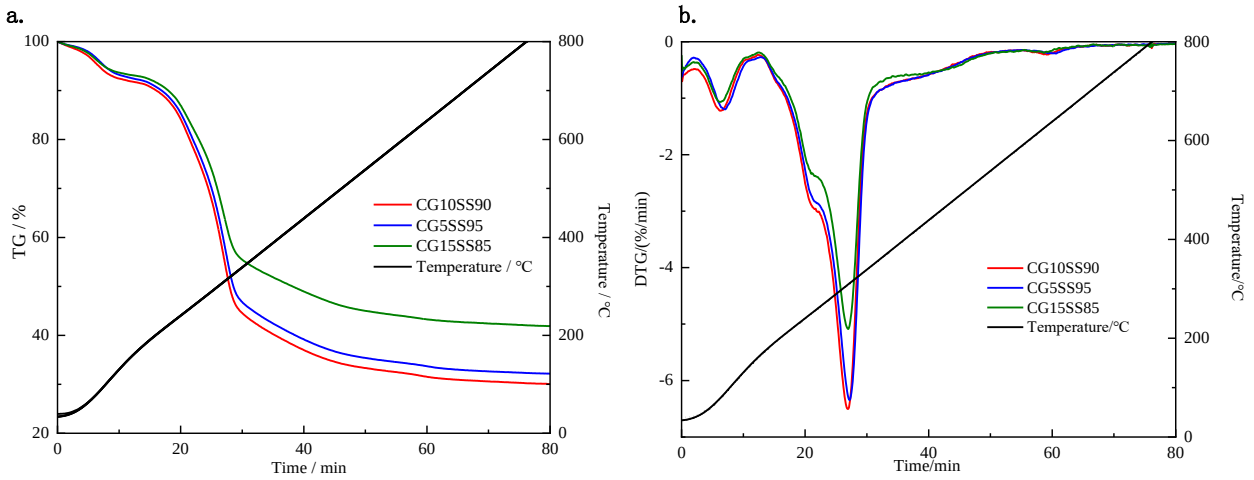

Figure 2. TG-DTG curves of the co-pyrolysis of coal gangue and biomass. **a.** TG curves. **b**. DTG curves.

content of biomass was much greater than that of gangue with both carbon content and H/C atomic ratio of 2.7 and 1.29 times more than that of gangue, respectively. With the increase of H atomic content, more H radicals were produced during pyrolysis process. This reflected low volatilization content, high pyrolysis temperature, low product yield, high biomass volatilization, low pyrolysis temperature, and high product yield of gangue. It was also shown that SS100 was easier to pyrolyze than CG100. Therefore, when coal gangue and biomass were co-pyrolyzed, more H free radicals were produced, promoting the synergistic relationship between them.

The co-pyrolysis TG-DTG curves of samples containing different gangue and biomass ratios were shown in Figure 2. During the mixed pyrolysis of gangue and biomass, the overall variation curve of TG-DTG was similar to that of SS100. In the DTG curves of CG10SS90, CG5SS95, and CG15SS85, main peak-to-peak temperature appeared at about 269, 272, and 270℃, respectively, which were almost the same as the peak temperature of SS100-DTG curve. The order of the intensity of the relationship between mass loss rate and weight loss degree was CG10SS90 > CG5SS95 > CG15SS85. Peak strength was related to mixture-to-mix ratio and the intensity of the main pyrolysis peak was increased by increasing biomass proportion. CG15SS85 curve presented a small variation and minimal quality loss. Co-pyrolysis mainly reflected the pyrolysis characteristics of biomass, while accelerating pyrolysis reaction speed and improving pyrolysis efficiency.

Characteristic analysis of main gases produced by the pyrolysis of coal gangue and biomass

Elemental and industrial analysis results indicated a high volatile mass fraction and low ash mass fraction for straw (Table 1). Biomass and gangue were mainly composed of C, H, and O elements and their related oxides were mainly generated during pyrolysis. The coal gangue exhibited a significant proportion of ash content. The total gas yields of coal gangue and biomass pyrolysis showed that co-pyrolysis effectively inhibited the precipitation of CO_2, CO, CH_4, H_2O, and H_2 gases. The total amounts of CO_2, CO, and CH_4 gases released during the pyrolysis process of CG15SS85 were 62.98, 52.82, and 61.9% lower than those of SS100, respectively (Figure 3).

Adsorption characteristics and surface morphology of biochar

Biochar microporous structure is an important factor that determines its performance [22]. According to the International Union of Pure Theoretical and Applied Chemistry (IUPAC) classification, pore structure can be classified as

Table 1. Proximate and elemental analysis of coal gangue and sunflower stalk.

Raw material	Industrial analysis (W/%)				Elemental analysis (W/%)						
	moisture	ash content	volatiles	fixed carbon	[C]	[H]	[N]	[O]	[P]	[S]	[Si]
Sunflower straw	4.93	6.16	85.25	3.66	40.67	5.51	0.31	35.51	0.01	0.07	7.26
coal gangue	2.44	77.55	17.94	2.07	15.06	1.57	0.18	8.71	0.06	0.18	25.13

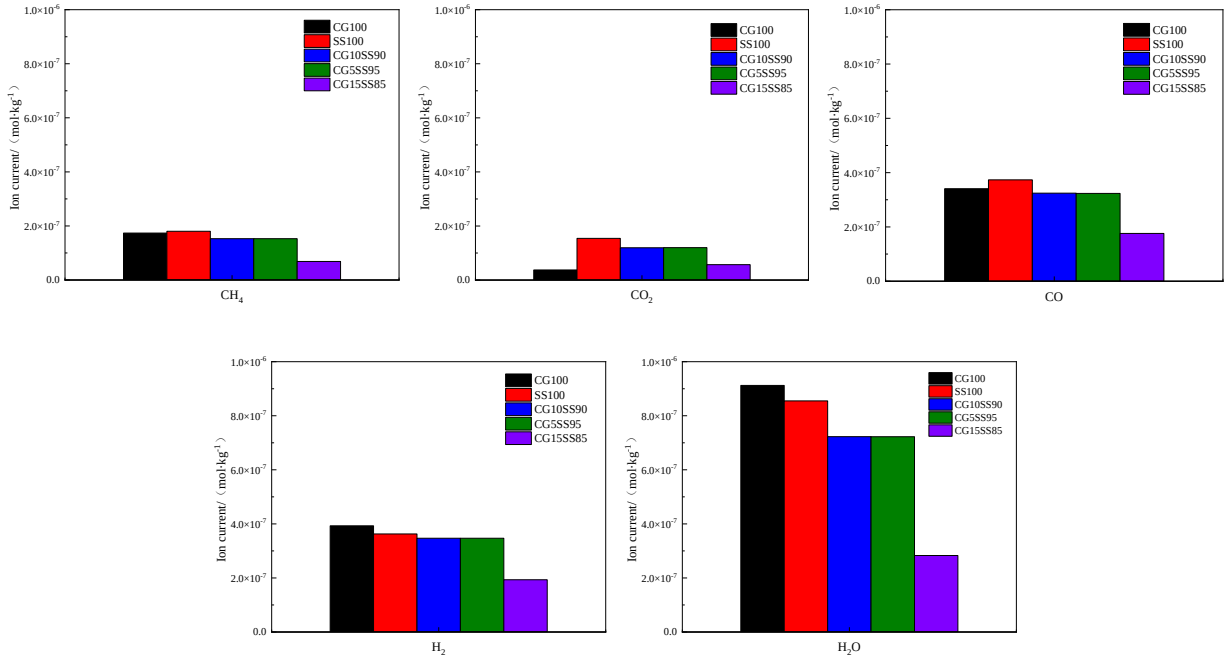

Figure 3. Total yields of coal gangue and biomass pyrolysis gases.

microporous, mesoporous, and macroporous with pore size less than 2 nm, 2 - 50 nm, and greater than 50 nm, respectively. Different pore structures present different adsorption mechanisms. Determination of specific surface area, pore size distribution, and pore volume by biochar adsorption-desorption using low-pressure N_2 or CO_2 gas is one of the most extensively applied methods. Generally, the specific surface area is obtained by BET model analysis and size distribution and volume of pores are calculated by BJH and DFT models, respectively. On this basis, specific surface area and pore volume of biochar were systematically analyzed and quantified. BJH model is suitable for the calculation of pore size distribution for pores greater than 2 nm in size, but results in large underestimation of pore volume with pore size less than 2 nm [23]. DFT model is more accurate for characterizing microwells [24].

(1) N_2 isothermal adsorption-desorption curve

IUPAC divides gas isothermal adsorption-desorption curves into six types. The shape of the biochar adsorption-desorption isotherm after the pyrolysis of gangue and biomass was similar to that of type I isotherm (Figure 4). The difference between desorption and adsorption curves was that, during adsorption process, relative pressure was increased, interlayer gap of biochar appeared, and N_2 entered the originally inaccessible pores under the action of external

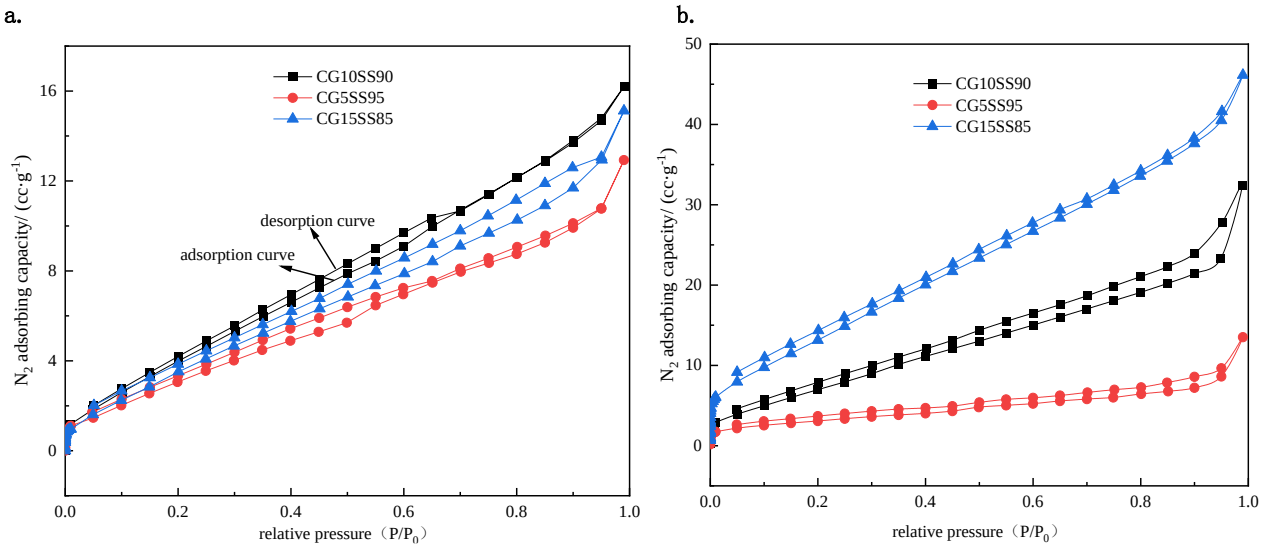

Figure 4. Isothermal adsorption curves of the co-pyrolysis of coal gangue and biomass. **a.** final pyrolysis temperature at 400°C. **b.** final pyrolysis temperature at 800°C.

force. When relative pressure was decreased, N_2 was sandwiched in the pores and was difficult for it to break away without external force, resulting in the misalignment of adsorption and desorption curves [25]. When relative pressure was low, N_2 adsorption increased rapidly, and curved isotherms appeared because micropore filling adsorption occurred in biochar and pore distribution was relatively concentrated. When relative pressures were between 0.2 and 0.9, adsorption capacity increased with the increase of relative pressure. Biochar pore monomolecules were close to saturation from adsorption. Multi-layer adsorption mainly occurred on the surface, indicating the presence of mesopores in biochar [23]. When relative pressure was larger than 0.9, capillary agglomeration occurred in pores, resulting in a sharp increase in adsorption capacity. When relative pressure approached 1.0, adsorption capacity was still increasing, indicating that biochar might contain a large number of mesopores or a certain number of large pores, resulting in a sharp increase in nitrogen uptake. At low temperature of 400°C with relative pressure of 1, CG10SS90 nitrogen adsorption capacity was the highest. Under high temperature conditions, pore adsorption capacity was much greater than that at low temperature and different treatments provided remarkably different results. At high temperature of 800°C and relative pressure of 1.0, CG15SS85 presented the highest adsorption capacity of 46.1445 mmol/kg, which increased the adsorption capacity by nearly 3 times compared to that at lower temperature (400°C), indicating that the adsorption capacity of biochar after high-temperature carbonization was greater and the adsorption capacity of CG15SS85 was about 3.42 times higher than that of CG5SS95.

(2) BJH pore size distribution curve

Mesoporous and macroporous models were calculated using the BJH model of N_2 adsorption curve. The pore size distributions and specific surface area of biochar according to BJH model showed that, by increasing pyrolysis temperature, pore size distribution showed complex changing trends and pore volume variation range was 0.00015 - 0.0299 cm^3/g under low-temperature condition. Pore size was mainly distributed in the range of smaller than 7.7 nm mesopores, indicating that a large number of mesopores were formed in low-temperature range, which was consistent with

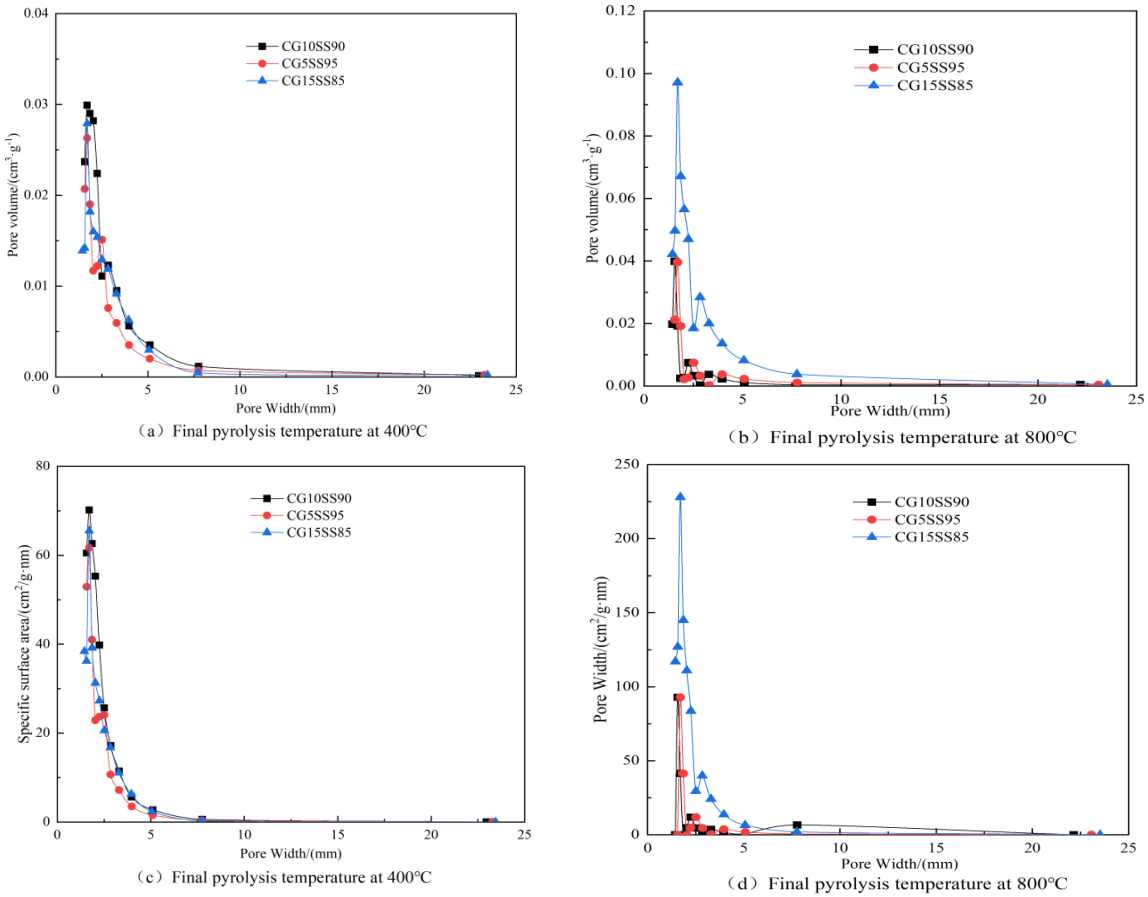

Figure 5. Pore size distribution characteristics of pore volume and specific surface area under BJH model.

adsorption isothermal curve (Figure 5). When pyrolysis temperature increased, pore volume change range was 0.0004114 - 0.0971 cm^3/g, and pore size distribution remained basically unchanged. It was found that the increase of temperature significantly increased the change range of pore volume, but pore size distribution was not obvious, because the formation of a large pore could be the sum of many small holes. For pore area, the trend was similar to that of pore volume, mainly due to the contribution of mesopores less than 7.7 nm in size.

(3) DFT pore size distribution curve

Micropore volume was obtained by DFT model. Due to relatively large errors in the measurement of micropores by N_2 adsorption method, CO_2 is usually applied as a molecular probe to characterize micropore structure. The results showed that the pore sizes were mainly distributed in the ranges of 0.6 - 0.9 nm and 1.1 - 1.6 nm at low temperatures. Increase of temperature resulted in more distribution of pore size in the intervals of 0.5 - 0.9 nm and 1.1 - 1.8 nm, therefore, increased micropore volume. The results confirmed that the pore volume span of CG15SS85 and the pore size distribution range of CG5SS95 (0.55-1.85 nm) were the largest (Figure 6). By combining BJH and DFT simulation methods, the biochar obtained by pyrolysis of gangue and biomass presented large amounts of microporous and mesoporous structures. Among them, the size of micropores were in the intervals of 0.5 - 0.9 nm and 1.1 - 1.8 nm. The mesopores were mainly distributed in the interval of less than 7.7 nm. At the high temperature, pores were more developed, showing a larger pore volume. CG5SS95 had a wider pore size range and

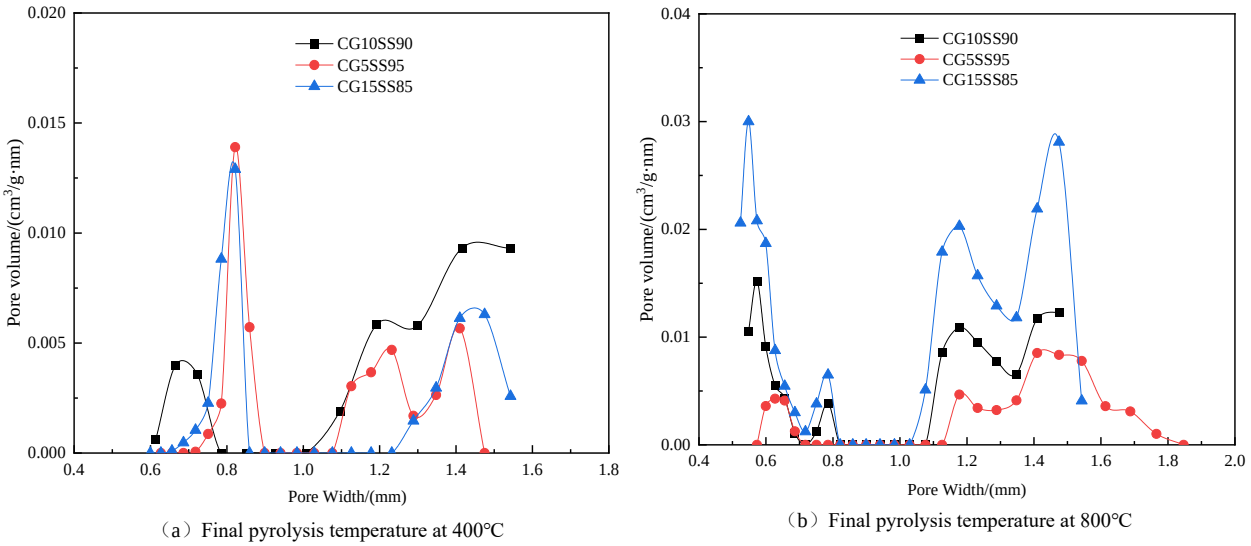

Figure 6. Pore size distribution characteristics of pore volume under BJH model.

Table 2. Pore parameters of biochar.

Parameter	CG10SS90		CG5SS95		CG15SS85	
	400℃	800℃	400℃	800℃	400℃	800℃
BET area (m^2/g)	26.59	40.166	14.714	19.029	24.405	74.378
Total pore body (cc/g)	3.43×10^{-2}	7.25×10^{-1}	2.94×10^{-2}	2.86×10^{-2}	3.20×10^{-2}	9.77×10^{-1}

larger pore volume at low temperature, while CG15SS85 performed better at high temperature. The change trends of pore volume and pore area were similar.

(4) Specific surface area

The specific surface area and pore volume of biochar were at low levels under low-temperature conditions (Table 2). By increasing pyrolysis temperature, specific surface area and pore volume were increased, but there was no obvious correlation between specific surface area and total pore volume. The specific surface area of CG15SS85 was increased by nearly 3.1 times from 24.405 to 74.378 m^2/g. The reason was that high-temperature pyrolysis changed the chemical composition and spatial structure of materials during conversion process and the number of micropores was increased, increasing specific surface area. This was the same as experimental conclusion of Song *et al*. [26]. High-temperature conditions were conducive to the development of pore structure in biochar, increasing pore volume and specific surface area.

(5) Surface morphology of biochar

Electron microscopy images intuitively reflected the surface morphology characteristics of biochar under different conditions. The SEM images of biochar under different conditions demonstrated that, under low-temperature condition, biochar structure was monolithic and flaky with a porous structure and pores. The quantities of different treatments were different. At high temperature, flaky pore structure collapsed. Pores became thinner with many scattered and disorderly block structures being formed, and relatively loose flocculation substances appeared on block structure surface (Figure 7). The surface morphology of the biochar samples prepared at different temperatures varied greatly, mainly because the thermal

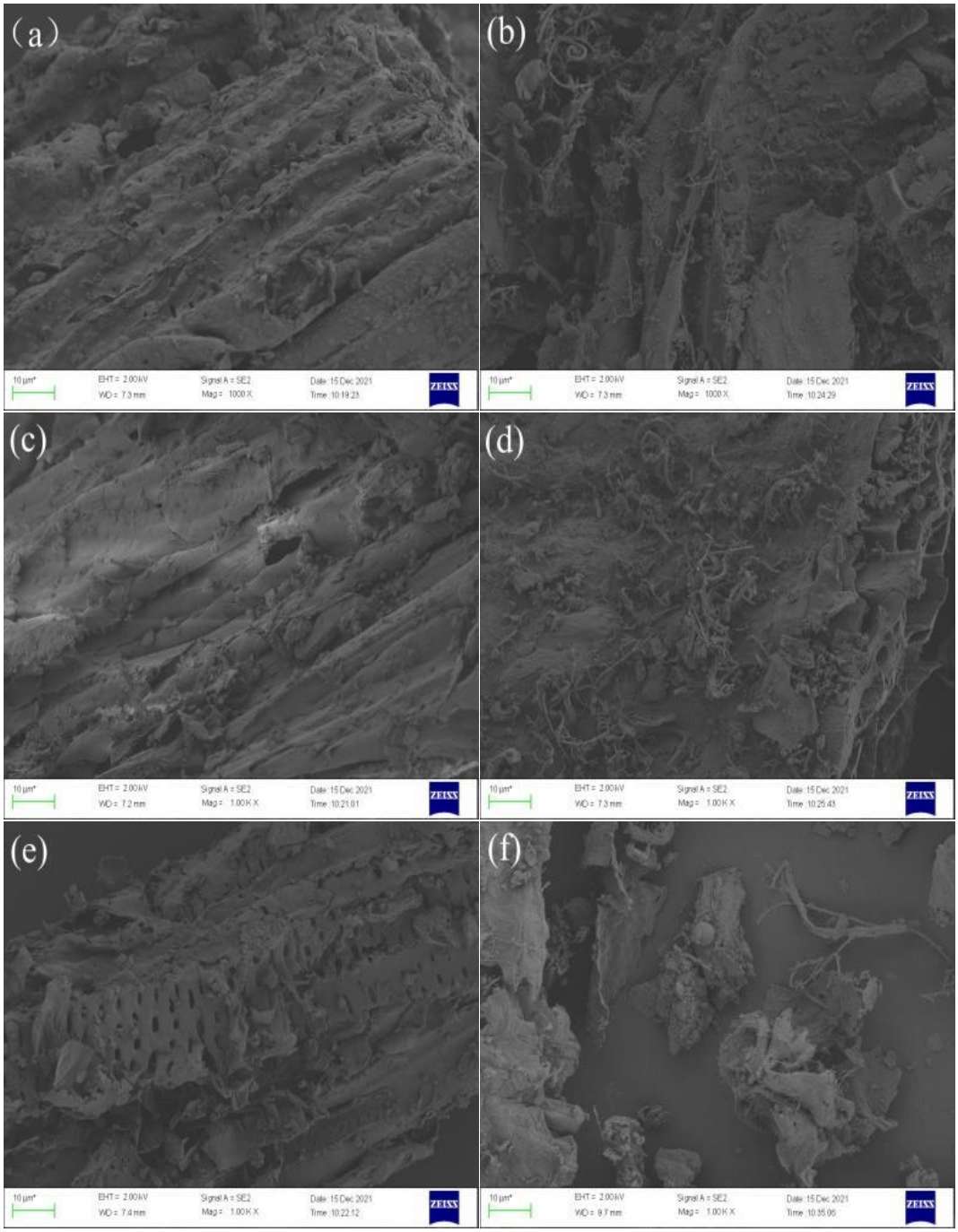

Figure 7. SEM images of biochar. Images a, c, e were the co-pyrolysis of CG10SS90, CG5SS95, and CG15SS85 at 400°C, respectively. Images b, d, f were the co-pyrolysis of CG10SS90, CG5SS95, and CG15SS85 at 800°C, respectively.

decomposition temperatures of tissue components such as cellulose, hemicellulose, lignin, and water contained in biomass were different, resulting in obvious porous structures of biochar at different temperatures, indicating that pyrolysis temperature was an important reason for biochar morphology variations. After co-pyrolysis of gangue and biomass, significant differences were observed in pore size and quantity, and their sheet structures were more

fragmented, which might be due to that the organic matter in biomass and oxide in gangue underwent redox reaction, causing combustion, thereby decomposing each other, resulting in many micropores left on biochar surface, which directly increased specific surface area. The performance effect became more obvious by increasing pyrolysis temperature.

Conclusion

In this research, variations of sample weight, structure, and pyrolysis gas of gangue, biomass, and different mixing ratios of biomass and gangue were examined. The results found that the main pyrolysis quality loss stage was the combustion stage of volatilization analysis. The peak intensity of curve corresponding to weightless region in DTG curve was related to blending ratio. With the increase of biomass proportion, the intensity of the main pyrolysis peak was increased, and the increase of temperature increased the degree of pyrolysis and mass loss. Co-pyrolysis effectively inhibited the precipitation of total gas. The total amounts of CO_2, CO, and CH_4 gases precipitated during the pyrolysis process of CG15SS85 were reduced by 62.98, 52.82, and 61.9%, respectively, compared to that of SS100. The biochar pore structure after the co-pyrolysis of gangue and biomass was dominated by micropores and mesopores less than 7.7 nm in size in the ranges of 0.5 - 0.9 nm and 1.1 - 1.8 nm. The pore volume was increased at high temperature. The change trends of pore volume and pore area were similar. The specific surface area of biochar was positively correlated with adsorption capacity and increase of temperature increased specific surface area, but there was no obvious correlation between specific surface area and total pore volume. The SEM images showed that biochar at high temperature had a more obvious pore structure than that at low temperature, and appropriately increasing pyrolysis temperature and gangue incorporation amount increased the number of pore structure in biochar.

Acknowledgements

This study was supported by Basic Research Funds for Universities Directly Affiliated to Inner Mongolia Autonomous Region (Grant No. BR22-15-03), Key Special Project of "Promoting Mongolia through Science and Technology Action" (Grant No. NMKJXM202310), Inner Mongolia Science and Technology Department (Grant No. 2021ZD0020), and Shandong Energy Institute (Grant No. SEI U202311).

References

1. Yang B, Peng L, Wang Y, Song J. 2018. The characteristics of air pollutants from the combustion of biomass pellets. Energ Source Part A. 40(3):351-357.
2. Li J, Wang J. 2019. Comprehensive utilization and environmental risks of coal gangue: A review. J Clean Prod. 239:117946.
3. Font O, Córdoba P, Leiva C, Romeo LM, Bolea I, Guedea I, *et al*. 2012. Fate and abatement of mercury and other trace elements in a coal fluidised bed oxy combustion pilotplant. Fuel. 95:272-281.
4. Liu Y, Xu Q. 2016. Characteristic analysis of chemical elements and pyrolysis of coal gangue in Ulan Mulun mining area. Coal Eng. 48(08):128-131.
5. Ran JY, Niu B, Zhang L, Pu G, Tang Q. 2006. Study on general combustion performance and kinetic characteristics of combustion of coal residue. In Zhongguo Dianji Gongcheng Xuebao (Proceedings of the Chinese Society of Electrical Engineering). 26(15):58-62.
6. Jin K, Zhang K, Ji Y, Lv H, Han G, Liu Y. 2020. Copyrolysis characteristics of coal and biomass at medium high temperatures. Therm Power Gen. 49(09):39-45.
7. Yang G, Jia X. 2018. A review on the mixed combustion of biomass and coal gangue. Ind Heating. 47(05):1-4.
8. Yuan YW, Tian YS, Zhao LX, Meng HB. 2012. The research process of the biochar application. Ke Zai Sheng Neng Yuan. 30(9):45-49.
9. Raveendran K, Ganesh A, Khilar KC. 1996. Pyrolysis characteristics of biomass and biomass components. Fuel. 75(8):987-998.
10. Alonso MJG, Borrego AG, Alvarez D, Kalkreuth W, Menendez R. 2001. Physicochemical transformations of coal particles during pyrolysis and combustion. Fuel. 80(13):1857-1870.
11. Wang B, Dong L, Wang Y, Matsuzawa Y, Xu G. 2010. Process analysis of lignite circulating fluidized bed boiler coupled with pyrolysis topping. In Proceedings of the 20th international conference on fluidized bed combustion (pp. 706-711). Springer Berlin Heidelberg.

12. Yusupov TS, Shumskaya LG. 2008. A thermal analysis study of the thermooxidative degradation of mechanically activated brown coal. Solid Fuel Chem+. 42(5):301-305.
13. Jin Z, Song C, Wang S, Wang R, Li R. 2015. The pyrolysis study of lignite (coal) and coal gangue. J Eng Thermophys-Rus. 36(01):7-10.
14. Wang S, Song C, Shen B. 2012. The pyrolysis study of lignite and coal gangue. Power Syst Eng. 28(05):11-13, 17.
15. Gong Z, Song C, Li Y. 2020. Effect of heating rate on combustion characteristics of biomass and coal gangue under O_2/CO_2 atmosphere. Acta Energiae Solaris Sinica. 41(09):366-374.
16. Pu G, Zhang L, Wang J, Ran J, Tang Q, Yan Y. 2009. Experimental study on co-combustion characteristics of biomass and coal residue. J Eng Phys. 30:333-335.
17. Bi H, Ni Z, Tian J, Jiang C, Sun H, Lin Q. 2022. Influence of lignin on coal gangue pyrolysis and gas emission based on multi-lump parallel reaction model and principal component analysis. Sci Total Environ. 820:153083.
18. Howaniec N, Smoliński A. 2013. Steam co-gasification of coal and biomass–Synergy in reactivity of fuel blends chars. Int J Hydrogen Energ. 38(36):16152-16160.
19. Wei S. 2017. Influence of biomass feedstocks and pyrolysis temperatures on physical and chemical properties of biochar. University of Chinese Academy of Sciences (Guangzhou Institute of Geochemistry, Chinese Academy of Sciences).
20. Lu J, Fu X, Kang J, Cheng M, Wang Z. 2021. Characterization of full pore and stress compression response of reservoirs with different coal ranks. Front Earth Sc-Switz. 9:764853.
21. Shen J, Xu J, Li Y. 2016. Study on measuring the pore diameter of powder by BJH method. Eng Technol. 2016(01):184-185.
22. Tsai WT, Liu SC, Chen HR, Chang YM, Tsai YL. 2012. Textural and chemical properties of swine-manure-derived biochar pertinent to its potential use as a soil amendment. Chemosphere. 89(2):198-203.
23. Du J. 2014. Study on preparation and physicochemical properties of Napa Lake Plateau Wetland biochar. Kunming University of Science and Technology.
24. Wang G. 2017. Theoretical computation on adsorption capacity of simple gas molecule for wooden activated carbon. Nanjing Forestry University.
25. Kondo S, Ishikawa T, Abe I. 2006. Chemical Industry Press. BeiJing: Chemical Industry Press. pp. 57-96.
26. Song W, Guo M. 2012. Quality variations of poultry litter biochar generated at different pyrolysis temperatures. J Anal Appl Pyrol. 94:138-145.